The TRPM4 inhibitor 9-phenanthrol activates endothelial cell $IK_{Ca}$ channels in rat isolated mesenteric artery

*C J Garland, [1]S V Smirnov, P Bagher, C S Lim, C Y Huang, R Mitchell, C Stanley, A Pinkney, K A Dora

Department of Pharmacology
University of Oxford
Mansfield Road
Oxford
OX1 3QT

*author for correspondence, email: christopher.garland@pharm.ox.ac.uk

1. Dr S V Smirnov, Department of Pharmacy and Pharmacology, University of Bath, Bath BA2 7AY,
email: S.V.Smirnov@bath.ac.uk

Author contributions:

CJG; conceived the study, acquired funding and reagents, performed the majority of experiments, analyzed data and wrote the manuscript
SVS; performed the patch clamp experiments and analyzed data, contributed to experimental design
PB; contributed to experimental design and the manuscript preparation
CSL; performed IHC experiments, contributed to manuscript preparation
CYH; RM, CS, AP; performed some of the experimental work
KAD; conceived the study, acquired funding and reagents, performed experiments, analyzed data, prepared figures and contributed to manuscript preparation

Abbreviations:

ACh (acetylcholine); EC (endothelial cell); NMDG (N-Methyl-D-glucamine); $IK_{Ca}$ (intermediate conductance calcium activated potassium channel); $SK_{Ca}$ (small conductance calcium activated potassium channel); SMC (smooth muscle cell); SUR (sulphonylurea receptor); TRAM-34 (1-[(2-Chlorophenyl)diphenylmethyl]-1*H*-pyrazole); TRPM4 (transient receptor potential melastatin 4 channel); TRPM5 (transient receptor potential melastatin 5 channel)

***Background and purpose***

Smooth muscle TRPM4 channels play a fundamental role in the development of the myogenic arterial constriction that is necessary for blood flow autoregulation. As TRPM4 channels are present throughout the vasculature, we investigated their potential role in non-myogenic resistance arteries using the TRPM4 inhibitor 9-phenanthrol.

***Experimental Approach***

Pressure and wire myography were used to assess artery reactivity, the latter in combination with measurements of smooth muscle membrane potential. Immunohistochemistry and endothelial cell (EC) calcium changes were assessed in pressurized vessels and patch clamp measurements made in isolated ECs.

***Key Results***

The TRPM4 inhibitor, 9-phenanthrol reversibly hyperpolarized mesenteric arteries to *circa* $E_K$ and blocked $\alpha_1$-adrenoceptor mediated vasoconstriction. Hyperpolarization was abolished and vasoconstriction reestablished by damaging the endothelium. In mesenteric and cerebral artery smooth muscle, 9-phenanthrol hyperpolarization was effectively blocked by the $IK_{Ca}$ inhibitor TRAM-34. 9-Phenanthrol did not increase mesenteric EC $[Ca^{2+}]_i$, and $Na^+$ substitution with N-Methyl-D-glucamine (NMDG) only increased the muscle resting potential by 10 mV. Immunolabelling for TRPM4 was restricted to the endothelium and perivascular tissue.

***Conclusions and Implications***

These data reveal a previously unrecognized action of the TRPM4 inhibitor 9-phenanthrol, the ability to activate EC $IK_{Ca}$ channels. They do not indicate a functionally important role for TRPM4 channels in the reactivity of non-myogenic mesenteric arteries.

## *Introduction*

Transient receptor potential melastatin 4 (TRPM4) channels are calcium-activated, non-selective cation channels. The channels are impermeable to $Ca^{2+}$ ions and have been suggested to play a fundamental role in cerebrovascular myogenic contraction. By conducting sodium, they are suggested to cause smooth muscle cell (SMC) depolarization, which opens voltage-gated calcium channels allowing $Ca^{2+}$ influx that then generates myogenic contraction (Earley *et al.*, 2007; Earley *et al.*, 2004). Evidence to support this suggestion was initially based on the use of TRPM4 antisense oligodeoxynucleotides, which suppressed both pressure-induced depolarization and myogenic constriction in cerebral arteries (Earley *et al.*, 2004). These observations were significantly extended by the use of the TRPM4 blocker, 9-phenanthrol (9-hydroxyphenanthrene). As well as blocking TRPM4 currents in dispersed SMCs, in cerebral arteries 9-phenanthrol reversibly hyperpolarized the vascular SMCs to *circa* -70 mV. This effect was correlated with a reduction in myogenic tone of around 75% (Gonzales *et al.*, 2010).

9-Phenanthrol was first identified as a selective TRPM4 blocker by screening different hydroxytricyclic compounds in HEK-293 cells expressing either TRPM4 or the closely related cation channel TRPM5 (Grand *et al.*, 2008). 9-Phenanthrol was subsequently shown to block TRPM4 channels with similar potency in native cells from a range of different tissues (Guinamard *et al.*, 2014). For example, in isolated cerebrovascular SMCs, 9-phenanthrol inhibited TRPM4 currents with an $IC_{50}$ in the low micromolar range, but did not affect the activity of a number of other types of ion channel (Gonzales *et al.*, 2010).

TRPM4 channels are widely expressed across a range of different tissues and, based on indirect studies, thought to be present in small mesenteric arteries (Weston *et al.*, 2013). In view of the proposed role of TRPM4 channels in myogenic contraction, we used the selective blocker 9-phenanthrol to investigate the potential role of these channels in mesenteric resistance arteries of a size that does not generate myogenic contraction. Although overall our data were similar to the reported effect of this agent in cerebral arteries, 9-phenanthrol appeared to evoke hyperpolarization by activating calcium activated $K^+$ channels ($K_{Ca}$) in the endothelium. In addition, these data do not indicate a functional role for TRPM4 channels in mesenteric resistance artery reactivity, but further emphasize the importance of $IK_{Ca}$ channels in regulating membrane potential and vascular tone.

## *Methods*

*Preparation of arteries for pressure or wire myography*

Animal use complied with the University of Oxford local ethical guidelines and the Animals (Scientific Procedures) Act 1986. Male Wistar rats (225-250g) were killed by cervical dislocation and exsanguination (as specified by Schedule 1 of the Animals (Scientific Procedures) Act 1986, UK). The mesenteric arcade was removed and placed in ice-cold MOPS buffer containing (mM): 145 NaCl, 4.7 KCl, 2 $CaCl_2$, 1.17 $MgSO_4 \cdot 7H_2O$, 2 MOPS, 1.2 $NaH_2PO_4 \cdot H_2O$, 5 glucose, 2 pyruvate, 0.02 EDTA, 2.75 NaOH with pH adjusted to 7.40 ± 0.02 (at 37ºC) with NaOH. A third-order segment of mesenteric artery (external diameter between 250-350 μm at 70 mmHg) with no visible side branches was dissected free of adherent tissue. After the artery was

mounted in either a pressure or wire myograph, reactivity was assessed by preconstriction with phenylephrine (PE, 0.5 - 3 μM) followed by endothelium-dependent relaxation to acetylcholine (ACh, 0.1 and 1 μM). Only vessels that relaxed by more than 95% were used further.

*Measurement of smooth muscle membrane potential*

Segments of mesenteric artery (2 mm) were mounted in a Mulvany-Halpern wire myograph (model 400A, Danish Myo Technology, Denmark) in Krebs solution containing (mM): 118 NaCl, 25 $NaHCO_3$, 3.6 KCl, 1.2 $MgSO_4 \cdot 7H_2O$, 1.2 $KH_2PO_4$, 2.5 $CaCl_2$, 11 glucose and gassed with 21% $O_2$, 5% $CO_2$, balance $N_2$ at 37ºC. The temperature was increased to 37ºC, and arteries normalized to a resting tension equivalent to that generated at 90% of the diameter of the vessel at 70 mmHg. Artery viability was then assessed as described above.

The SMC membrane potential was measured using sharp glass microelectrodes backfilled with 2 M KCl (tip resistances *circa* 100 MΩ), as previously described (Garland & McPherson, 1992; Garland *et al.*, 2011b). Membrane potential was recorded through a pre-amplifier (Neurolog system, Digitimer Ltd., U.K.) linked to a MacLab data acquisition system (AD Instruments Model 4e, usually at 100 Hz). All drugs were added directly to the bath or, in the case of NMDG, substituted for $[Na^+]_o$ in the Krebs solution.

*Measurement of endothelial cell membrane potential*

For patch clamp studies, ECs were isolated from mesenteric arteries that had been cut open and placed in nominally $Ca^{2+}$-free physiological saline solution (HEPES-PSS) containing (mM): 130 NaCl, 5 KCl, 1.2 $MgCl_2$, 10 glucose, 10 HEPES (pH adjusted to 7.40 ± 0.02 with NaOH) with the additional presence of 1 mg/ml papain, 1 mg/ml bovine serum albumin (BSA, fraction V) and 1 mg/ml dithiothreitol for 10 min at room temperature and then for 30 min at 36ºC. The arteries were then washed in $Ca^{2+}$-free BSA-containing HEPES-PSS and gently triturated to release ECs. Cell suspensions were stored on ice (the $Ca^{2+}$ concentration was gradually increased to 0.5 mM) and used on the same day. All patch clamp recordings were performed in HEPES-PSS containing 1 mM $CaCl_2$. The recording pipette solution contained (mM): 140 KCl, 2 MgATP, 0.1 $Na_2GTP$, 0.5 $MgCl_2$, 10 HEPES, 0.1 EGTA, pH adjusted to 7.20 with KOH.

Membrane potential was recorded from EC sheets (containing between 3 and >20 cells, mean 13 ± 2, n=25) using the current clamp mode of the whole-cell patch clamp technique at sampling rate 10 Hz (Axoclamp 200B amplifier; Axon Instruments, Union City, CA, USA). Pipette resistance, when filled with pipette solution, was 5-10 MΩ.

*Measurement of endothelial $[Ca^{2+}]_i$ changes*

Arteries were cannulated with two glass micropipettes in a temperature-regulated chamber (2 mL, Warner Instruments) placed on the stage of an inverted microscope (FluoView500 linescan confocal, Olympus, Japan) as previously described (Kansui *et al.*, 2008). Following equilibration and testing arterial function the ECs were selectively loaded with $Ca^{2+}$ indicator dye. Briefly, the intraluminal pressure was lowered to 4 mmHg and the artery perfused with MOPS buffer containing 0.02%

Pluronic F-127 and the cell-permeable $Ca^{2+}$ dye Oregon Green 488 BAPTA-1 AM (OGB-1, 10 μM, 30 min) (Kansui *et al.*, 2008). After the dye was washed out of the lumen with MOPS buffer, the pressure was increased and the artery left for another 30 min to allow de-esterification. Arteries were then excited at 488 nm and emitted light collected at >505 nm with a 40x water immersion objective (UApo N340, Olympus, Japan). ECs were visualized in a clip box of 472x144 pixels allowing a scan frequency of ~3 Hz. Cells (6-10 cells) were selected and fluorescence intensity was determined off-line using MetaMorph software (v.7.7.4, Molecular Devices, USA). Subcellular regions of interest (diameter ~ 2 μm) were manually positioned within each EC, and the $Ca^{2+}$ events counted to obtain a frequency of events per cell per minute. Only active cells were included in the average. Results are also presented for the % active cells. All agents were added to the bath.

*Immunohistochemistry*

Immunohistochemistry was performed in pressurized arterioles as described previously (Bagher *et al.*, 2012; Dora *et al.*, 2008). In brief, arterioles were fixed in 2% (wt/vol) paraformaldehyde for 10 min at 37°C, washed with PBS, and incubated in blocking buffer (luminal and abluminal, 1% BSA and 0.1% Tween 20, pH 7.1) for 60 min at 37°C, then overnight with primary antibody at 4°C. Primary antibodies were as follows: 1:200 rabbit polyclonal anti-rat TRPM4 (aa 1110–1160; Abcam, ab63080); 1:100 rabbit polyclonal anti-mouse connexin 40 (aa 340–358; Chemicon International, AB1726). The following day, the bath solution was replaced with PBS, and the lumen was perfused with Alexa Fluor 488 secondary antibody (1:100 chicken anti-rabbit IgG, Life Technologies, A-21441; or for connexin 40, 1:100 goat anti-rabbit IgG, Life Technologies, A-11034), and incubated for 2 h at room temperature. When double immunolabelling was performed, a 3 day protocol was used whereby the artery was imaged for TRPM4 expression prior to incubation with the Cx40 Ab and secondary Ab. Nuclei and elastin (including the IEL) were labelled with 15 μM propidium iodide and 200 nM Alexa Fluor 633 hydrazide (Life Technologies, A-30634), respectively. Arteries were excited at 488, 543, and 633 nm; the fluorescence emitted at 505–540 (GaAsP detector), 560–620, and 655–755nm was acquired through a water immersion objective (40x, NA 1.15; Olympus, 1,024 x 1,024 pixels, sequential scanning) by using an Olympus FluoView1200 microscope (Olympus, Japan). z-Stacks through the artery wall were obtained at 0.5 μm increments with Fluoview Software (FV10-ASW 4.1; Olympus) and reconstructed in Imaris Software (Version 7.7.1; Bitplane).

*Measurement of cerebral artery diameter*

Middle cerebral arteries were cannulated with two glass pipettes in a temperature-regulated chamber (10 mL, MOPS buffer, 120CP, Danish Myo Technology, Denmark) placed on the stage of an inverted microscope (IX71, Olympus, Japan) as previously described (Yuill *et al.*, 2011). The preparations were then warmed to 37°C, and pressure, driven by custom-built gravity-fed inflow and outflow system, was gradually increased to 80 mmHg. Arteries were visualized using a 10x/0.25 Olympus objective and video camera (C7500-51, Hamamatsu Inc, Japan) and vessel diameter changes tracked at 2 Hz using Diamtrak Edge-tracking software (v3.5, Diamtrak, Adelaide, Australia). All experiments were performed in the absence of intraluminal flow. Arteries developed spontaneous myogenic tone within ~30 min, and EC-function tested as dilation to ~95% of maximum diameter following addition of SLIGRL (protease-activated receptor 2 ligand, 10 μM) or ADPβS (3 μM).

*Data analysis*
Data were analyzed using Microsoft Excel 2011 (Microsoft Corporation) and GraphPad Prism (v5.0, GraphPad Software, USA) software. Dilation was expressed as a percentage reversal of tone induced by PE (100% corresponding to the maximal diameter). Results are summarized as mean ± S.E.M. of *n* replicates, where *n* is the number of individual arteries, each obtained from a separate animal. Statistical analyses were performed using Student's paired *t*-test or one-way ANOVA analysis followed by Bonferroni post-test. A value of $P < 0.05$ was considered to be statistically significant.

*Drugs and solutions*
All drugs were obtained from Sigma (UK) with the exception of apamin (Latoxan, France), levcromakalim (Tocris, UK) and OGB-1 (Life Technologies, UK). TRAM-34 (1-[(2-chlorophenyl)diphenylmethyl]-1*H*-pyrazole), 9-phenanthrol (9-hydroxyphenanthrene) and glibenclamide were dissolved in dimethyl sulfoxide, levcromakalim in ethanol. All other stock solutions were prepared using purified (MilliQ) water. All stock solutions were prepared at $10^{-2}$ M, except for L-NAME ($10^{-1}$ M), and subsequently diluted in MOPS buffer (pressurized arteries) or Krebs buffer (wire myograph). Inhibitors were pre-incubated with the arterial tissue for at least 20 min before agonist application.

## *Results*

*Smooth muscle hyperpolarization to the TRPM4 blocking agent 9-phenanthrol and the influence of K channel blockers*
9-Phenanthrol (20 μM) was previously shown to block TRPM4 current in native cerebral artery SMCs (Gonzales *et al.*, 2010) and in intact mesenteric arteries it stimulated a robust SMC hyperpolarization, which was both reversible and reproducible (Figure 1A, i-ii). The hyperpolarization to 9-phenanthrol was concentration-dependent, ranging from 1.9 ± 0.6 mV with 5 μM (n=5) to a maximum of 26.5 ± 1.2 mV (n=10) with 20 μM 9-phenanthrol (from a resting potential of -54.4 ± 1.2 mV).

Hyperpolarization to 20 μM 9-phenanthrol was effectively abolished by the $IK_{Ca}$ inhibitor, 1 μM TRAM-34, which reduced the hyperpolarization to 4.1 ± 1.5 mV (n=4) (Figure 1C). The effect was similar in the additional presence of the $SK_{Ca}$ blocker, 100 nM apamin (2.5 ± 1.0 mV, n=7), while alone apamin did not reduce hyperpolarization to 9-phenanthrol (28.7 ± 3.0 mV, n=4) (Figure 1C). In the continued presence of TRAM-34, apamin and 9-phenanthrol, the opener of $K_{ATP}$ channels 5 μM levcromakalim was still able to hyperpolarize to near $E_K$ (from -59.0 ± 2.6 to -82.4 ± 4.4 mV, n=5). Some attenuation of hyperpolarization to 9-phenanthrol was recorded in the presence of the $K_{ATP}$ blocker, 5 μM glibenclamide (to 20.1 ± 1.4 mV, $P < 0.05$, n=5) (Figure 1B).

The possibility 9-phenanthrol might cause hyperpolarization by block of a depolarizing $Na^+$ conductance was probed by replacing $[Na^+]_o$ with NMDG. This increased SMC resting membrane potential by around 10 mV, to -63.7 ± 1.5 mV, $P < 0.05$, n=10 (Figure 1D).

**Figure 1**

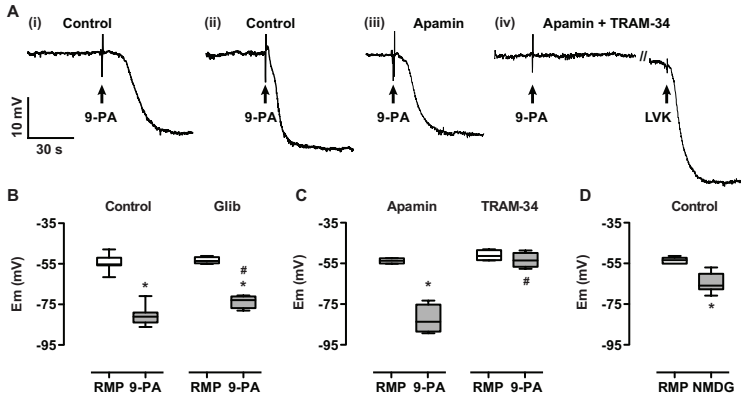


Effect of 9-phenanthrol on the smooth muscle membrane potential of mesenteric arteries and block with TRAM-34. Panel A, (i-ii) intracellular records showing reproducible and reversible hyperpolarization to 20 μM 9-phenanthol (9-PA) in the same preparation (iii) which, in a separate preparation, was unaffected by the presence of 100 nM apamin, (iv) but blocked in the additional presence of 1 μM TRAM-34. Under these conditions, hyperpolarization was subsequently evoked with 5 μM levcromakalim (LVK). Panel B-D, box and whisker plots summarizing (B) the effect of 20 μM 9-phenanthrol against resting membrane potential (RMP, left panel, n=10) and in the presence of 5 μM glibenclamide (Glib, n=5), (C) lack of block with 100 nM apamin alone and block with 1 μM TRAM-34 alone (n=4 in each case), (D) the effect of $[Na^+]_o$ replacement with NMDG on the resting membrane potential (n=10). *, $P < 0.05$ *vs* RMP; $^{\#}$, $P < 0.05$ *vs* Control 9-PA.

*The effect of 9-phenanthrol against smooth muscle membrane potential and vasoconstriction in endothelium damaged mesenteric arteries*

In mesenteric arteries in which the endothelium had been damaged with a human hair (-EC), neither ACh (0.1 - 3 μM, n=3) nor 9-phenanthrol (20 μM, n=5) changed the SMC resting membrane potential (of -47.9 ± 2.5 mV, n=5), but robust hyperpolarization was still evoked by the subsequent addition of 5 μM levcromakalim (to around $E_K$, Figure 2A). During hyperpolarization to 20 μM 9-phenanthrol in +EC arteries, both the depolarization and contraction normally evoked by the $\alpha_1$-

adrenoceptor agonist phenylephrine was blocked (Figure 2B). Phenylephrine contractile responses in the presence of 9-phenanthrol were restored in -EC arteries (Figure 2B).

**Figure 2**

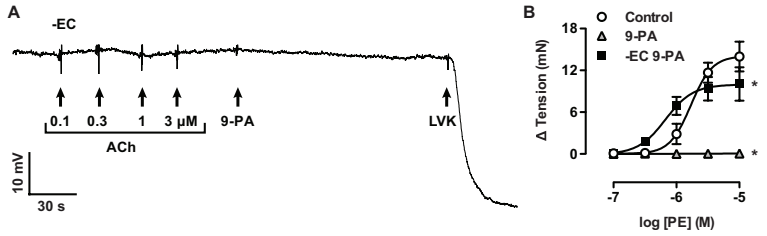


Damage to the endothelium (-EC) abolished hyperpolarization to acetylcholine and 9-phenanthrol but not to levcromakalim. Panel A, intracellular recording showing no hyperpolarization to 0.1 – 3 µM acetylcholine (ACh) or 20 µM 9-phenanthrol (9-PA), while the addition of the $K_{ATP}$ channel activator, 5 µM levcromakalim (LVK) evoked pronounced hyperpolarization to *circa* $E_K$. Panel B, concentration-response curves showing control contraction to phenylephrine (PE) is abolished in the presence of 20 µM 9-phenanthrol but reestablished in endothelium-damaged arteries in the presence of 9-phenanthrol (n=3 in each case). *, $P < 0.05$ *vs* Control.

*Endothelial cell calcium events*

ECs *in situ* in pressurized mesenteric arteries displayed spontaneous $Ca^{2+}$ events at a frequency of 2.1 ± 0.5 per active cell per min in 34 ± 1.0% of cells (n=3). This increased to 14.6 ± 3.1 per active cell per min in 86.2 ± 7.8% of cells during

stimulation with 0.3 μM ACh (n=3). 9-Phenanthrol reversibly blocked the EC $Ca^{2+}$ response to ACh but did not alter spontaneous basal $Ca^{2+}$ activity (Figure 3).

**Figure 3**

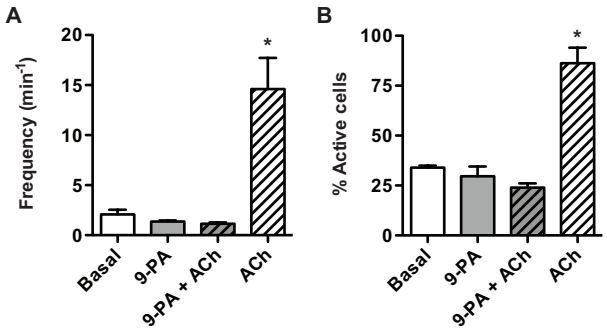


Measurement of endothelial cell calcium events and active cells in pressurized mesenteric arteries. 20 μM 9-phenanthrol (9-PA) did not alter basal $Ca^{2+}$ event frequency or the number of active cells, but blocked the ability of 0.3 μM ACh to stimulate events (n=3). *, $P < 0.05$ *vs* Basal.

*Hyperpolarization to 9-phenanthrol in isolated endothelial cell sheets*

Under conditions of current clamp, isolated EC sheets had a resting membrane potential of -10.9 ± 1.4 mV, n=25. Application of a sub-maximal concentration of 9-phenanthrol (5 μM) reversibly hyperpolarized EC sheets (to *circa* $E_K$, -75.6 ± mV, n=4) (Figure 4). TRAM-34 (1 μM) reduced this hyperpolarization by 44% (to -32.6 ±

5.2 mV, $P < 0.05$, n=4) (Figure 4B). The low EC resting potential appeared to be due to a $[Na^+]_o$ conductance, as NMDG reversibly increased the EC resting membrane potential to -57.5 ± 4.7 mV, n=11 (Figure 4C).

**Figure 4**

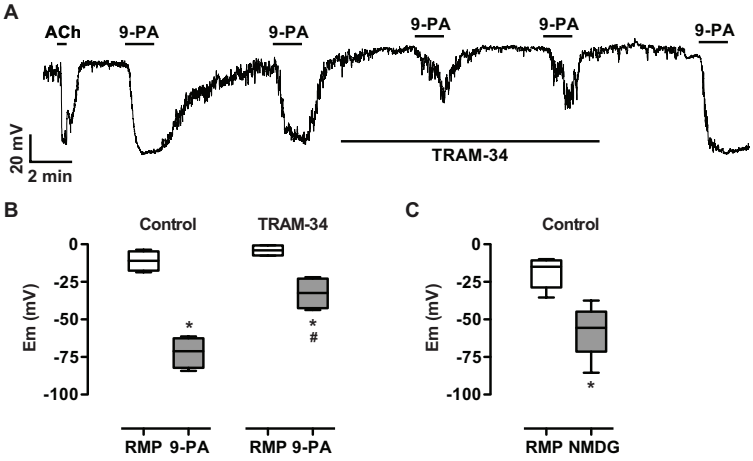


Current clamp recording from dispersed mesenteric artery EC sheets. Panel A, original trace showing reproducible and reversible hyperpolarization to 5 µM 9-phenanthrol, reduced in the presence of 1 µM TRAM-34. Panel B, box and whisker plot of paired data summarizing hyperpolarization to 5 µM 9-phenanthrol and reduced hyperpolarization (right panel) in the presence of 1 µM TRAM-34 (n=4 EC sheets). Panel C, summary of the hyperpolarization to superfusate containing NMDG (n=11 EC sheets). *, $P < 0.05$ *vs* RMP; $^{\#}$, $P < 0.05$ *vs* Control 9-PA.

*Immunohistochemical profile for TRPM4 in mesenteric arteries*

No immunolabelling with TRPM4 antibody was observed in mesenteric artery SMCs. However, both endothelium and the perivascular plexus were labelled by the TRPM4 antibody (Figure 5).

**Figure 5**

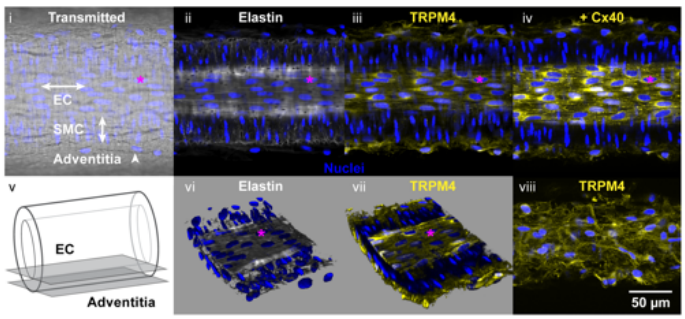


Confocal imaging in pressurized mesenteric arteries indicating TRPM4 antibody in endothelium and adventitia. **i.** Transmitted light image showing the relative alignment of endothelial cells (EC) and smooth muscle cells (SMC). Nuclear labelling (blue) with propidium iodide. **ii.** A merged image from the same artery (of five 0.5-µm z-axis planes) at the level of the internal elastic lamina (Elastin, white), focal plane EC in panel v. **iii.** Diffuse expression of TRPM4 (yellow) is apparent in the endothelium but absent from the SMCs. **iv.** Subsequent immunolabelling of the same artery for connexin 40 (yellow) using the same settings as iii, was restricted mainly to EC borders. **v.** Cartoon indicating the focal plane imaged for endothelial cells (EC) and shown in panels i-iv, and for adventitia shown in panel viii. **vi.** Reconstructed z-stacks, luminal surface upmost, showing alignment of SMCs approximately at right angles to the overlying ECs. **vii.** The same reconstructed z-stack including signal (yellow) indicating TRPM4 in the endothelium but absent from the SMC. **viii.** TRPM4 was also apparent at the level of the adventitia. Scale bar 50 µm applicable to all images. The pink asterisk marks the same nucleus in panels i-iv and vi-viii.

*Effect of 9-phenanthrol in middle cerebral arteries*

Isolated middle cerebral arteries mounted under isometric conditions developed myogenic tone and depolarization superimposed by spontaneous spike potentials. Myogenic tone and spike potentials were inhibited by the application of 1 μM nifedipine. The subsequent application of 20 μM 9-phenanthrol increased the resting membrane potential (-42.1 ± 1.0 mV) by 17.2 ± 1.8 mV (n=4). The increase was reduced to 5.5 ± 1.2 mV in the presence of TRAM-34 ($P < 0.05$, n=4) (Figures 6A & B). In pressurized arteries, which developed myogenic tone (maximum inner diameter 219 ± 4 μm, 44 ± 2% myogenic tone), 9-phenanthrol caused a rapid vasodilation and TRAM-34 markedly reduced the rate of vasodilation (Figure 6C). TRAM-34 did not markedly affect myogenic tone (50 ± 3%, n=3).

**Figure 6**

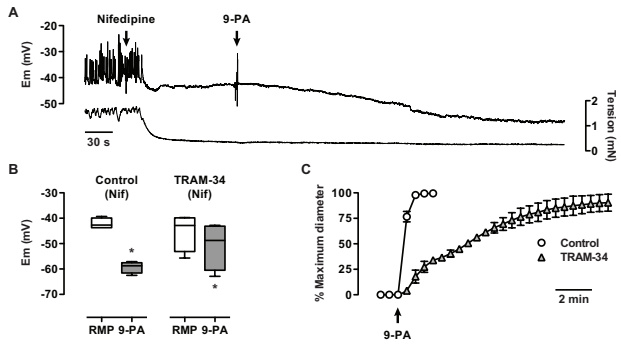


Inhibition of 9-phenanthrol hyperpolarization and vasodilation in middle cerebral arteries by TRAM-34. Panel A, intracellular recording of smooth muscle membrane potential in a tensioned middle cerebral artery. Spontaneous depolarization and contraction is blocked with 1 μM nifedipine. 20 μM 9-phenanthrol then causes hyperpolarization. Panel B, box and whisker plot to summarize the ability of 20 μM 9-phenanthrol to raise membrane potential (left panel), and (right) reduced in the presence of 1 μM TRAM-34, n=4. Panel C, vasodilation to 20 μM 9-phenanthrol in pressurized cerebral arteries is slowed but not diminished by the presence of 1 μM TRAM-34, n=3. *, $P < 0.05$ *vs* RMP.

***Discussion***

There are three major outcomes from the present study. In spite of the accepted selectivity of 9-phenanthrol for TRPM4 channels, we provide evidence to show first that it can also activate $IK_{Ca}$ channels, which in vascular tissue are focused within the endothelium; and second can block the acetylcholine-mediated increase in EC $Ca^{2+}$; each of these effects being reversible. Third, taken together our data are not consistent with a functional role for TRPM4 channels in mesenteric artery reactivity, certainly in non-myogenically active arteries.

9-Phenanthrol is the most selective TRP ligand currently available for TRPM4 channels, and appears not to affect the closely related TRPM5 channel even in concentrations as high as 100 μM (Grand *et al.*, 2008). Since this characteristic was first described, 9-phenanthrol has also been shown to lack activity against a range of other ion channels (summarized in Guinamard *et al.*, 2014). In myogenically active cerebral arteries, these include $BK_{Ca}$, $K_v$, $K_{ir}$ and voltage-dependent $Ca^{2+}$ channels (Gonzales *et al.*, 2010). Furthermore, while 9-phenanthrol abolished TRPM4 currents in cerebral SMCs, it had no effect against the currents mediated by either TRPC3 or TRPC6 channels (expressed in HEK-293 cells). The latter channels are present in cerebral SMCs and have been implicated in constrictor responses. In EC-intact cerebral arteries, 9-phenanthrol hyperpolarized the SMCs by *circa* 30 mV, increasing the membrane potential to values close to $E_K$. Based on the specificity of 9-phenanthrol described above, this effect was attributed to block of an ongoing SMC depolarization generated by TRPM4 channels.

In the present study, 9-phenanthrol evoked SMC hyperpolarization of similar magnitude and potency as reported in the earlier experiments with isolated cerebral arteries. However, the hyperpolarization in mesenteric artery SMCs did not appear to reflect a block of TRPM4 currents, but rather the activation of endothelial $IK_{Ca}$ channels, as it was abolished either by the specific $IK_{Ca}$ channel blocker TRAM-34 or by damage to the endothelium. In contrast, hyperpolarization was unaffected by the presence of apamin, which selectively blocks $SK_{Ca}$ channels, the second form of $K_{Ca}$ channel in the endothelium. Activation of both $IK_{Ca}$ and $SK_{Ca}$ channels in the endothelium underpins endothelium-dependent hyperpolarization (EDH) in both rat mesenteric and middle cerebral arteries (McNeish *et al.*, 2006). EDH is responsible for the nitric oxide independent vasodilation in small resistance arteries/arterioles, and is the predominant endothelium-dependent response leading to vasodilation in these small arteries (Garland *et al.*, 2011a).

Glibenclamide also suppressed hyperpolarization to 9-phenanthrol. Although the effect was modest, at *circa* 6 mV, it was significant. Functional TRPM4 channels, in contrast to TRPM5 channels, are glibenclamide-sensitive, and also subject to complex modulation by intracellular ATP (Demion *et al.*, 2007; Nilius *et al.*, 2005). How glibenclamide inhibits TRPM4 channels is not clear, but an obvious possibility is that it is acting on sulphonylurea receptors (SUR). SUR1 has been suggested to associate with TRPM4, to form SUR1-TRPM4 channels that are up-regulated acutely following CNS trauma and underlie the subsequent necrotic cell death (Woo *et al.*, 2013).

However, the ability of SUR-1 and TRPM4 to associate and form channels has been questioned (Sala-Rabanal *et al.*, 2012), but this discrepancy might simply reflect differing experimental conditions, because inhibition of SUR1-TRPM4 channels by glibenclamide reduces both neuroinflammation and the cognitive deficits that follow subarachnoid haemorrhage (Tosun *et al.*, 2013). The fact that SUR1-TRPM4 channels have not been reported to be constitutively expressed, and that we failed to detect significant immunohistochemical signal for TRPM4 in mesenteric SMCs, suggests that similar channels probably do not explain the attenuated hyperpolarization that we recorded with glibenclamide. However, 9-phenanthrol and related phenanthrene derivatives inhibit a number of protein kinases, so perhaps they somehow affect the ATP-binding site (Wang *et al.*, 1994).

How 9-phenanthrol activates EC $IK_{Ca}$ channels is not clear. This effect is not the result of an increase in EC $[Ca^{2+}]_i$, because neither event frequency nor the number of active cells was altered by 9-phenathrol. In fact, 9-phenanthrol reversibly blocked the ability of ACh to increase EC $[Ca^{2+}]_i$, events, indicating it disrupts cellular calcium handling, at least in the endothelium. This suggestion is consistent with the 'recovery' of phenylephrine-evoked contraction observed after EC damage, and strengthens the conclusion that the effect of 9-phenanthrol in mesenteric arteries is restricted to the endothelium. As a fused heteroaromatic structure, 9-phenanthol is a flat, rigid molecule. It shares these characteristics with the positive modulators of $K_{Ca}$ channels, which are based on the structure of EBIO (1-ethyl-2-benzimidazolinone), such as NS309 and the benzothiazole SKA-31. These molecules are either completely aromatic or contain single bonds that will allow rotation and enable the molecule to form a flat structure. $K_{Ca}$ channel activators appear to bind within the channel C-terminal region, close to the calmodulin binding site. In contrast, channel blockers such as the clotrimazole derivative TRAM-34 are larger and less likely to assume a flat structure. They bind in the outer vestibular region of $IK_{Ca}$ (Wulff & Kohler, 2013).

In the middle cerebral artery, hyperpolarization to 9-phenthantrol also appeared largely due to activation of $IK_{Ca}$. However, consistent with a functional role for TRPM4 in the cerebral arteries, block of $IK_{Ca}$ did not inhibit cerebral artery dilation, but it did slow the rate at which dilation developed. A recent study, in which 9-phenanthrol evoked cerebral artery dilation in endothelium-denuded vessels, is consistent with these observations (Cipolla *et al.*, 2014). In the same study, 9-phenanthrol also evoked SMC hyperpolarization, but these (separate) recordings appeared to be from endothelium-intact arteries. Cerebral artery hyperpolarization to 9-phenanthrol was proposed to arise due to block of a depolarizing sodium current (Gonzales *et al.*, 2010). However, while it seems clear that TRPM4 channels are important for cerebral myogenic tone, our data question this explanation.

In contrast to cerebral arteries, data from non-myogenic mesenteric arteries do not support a functional role for TRPM4 channels, at least in terms of arterial reactivity. Crucially, the hyperpolarization evoked with 9-phenanthrol was endothelium-dependent and appeared to reflect a direct activation of $IK_{Ca}$ channels. These data were supported by an absence of TRPM4 immunolabelling in the SMC layers and patch clamp measurements in ECs, which also showed hyperpolarization with 9-phenanthrol to be TRAM-34 sensitive. Also consistent are data from experiments in which $[Na^+]_o$ was replaced with non-permeant NMDG. This only increased resting membrane potential by 10 mV and contrasted with a *circa* 30 mV increase to 9-

phenanthrol. NMDG also hyperpolarized isolated ECs, and interestingly to close to the value of resting membrane potential recorded in intact arteries. The latter suggesting that the depolarized EC resting potential reflects a sodium-dependent process. Whether or not that involves EC TRPM4 channels is not clear, but whatever the mechanism, it does not seem to have any important influence on arterial reactivity. Previous research has shown that dissociated ECs are depolarized, and this is thought to reflect the fact that *in situ* the EC resting membrane potential is dominated by the more hyperpolarized SMC resting potential, reflecting heterocellular gap-junction coupling between the two cell types (Yamamoto & Suzuki, 2005).

In summary, our data do not support a role for TRPM4 channels in the reactivity of non-myogenic mesenteric arteries. They do reveal previously unrecognized effects of 9-phenanthol, the ability to activate EC $IK_{Ca}$ channels and as a result generate arterial hyperpolarization and relaxation, and to block acetylcholine-mediated EC $Ca^{2+}$ activity. These actions of 9-phenantrol should be considered whenever this agent is used as a probe for TRPM4 activity in intact arteries.

***Acknowledgments***

This research was supported by a Wellcome Trust Programme Grant. CJG holds a Royal Society-Wolfson Merit Award, KAD is a BHF Senior Basic Science Research Fellow. We are very grateful to Associate Professor Grant Churchill for helpful discussions about the structure of 9-phenanthrol and K channel ligands, and for equipment funds from the Oxford BHF Centre of Research Excellence.

***References***

Bagher, P, Beleznai, T, Kansui, Y, Mitchell, R, Garland, CJ, Dora, KA (2012) Low intravascular pressure activates endothelial cell TRPV4 channels, local $Ca^{2+}$ events, and IKCa channels, reducing arteriolar tone. *Proc Natl Acad Sci U S A* **109:** 18174-18179.

Cipolla, MJ, Chan, SL, Sweet, J, Tavares, MJ, Gokina, N, Brayden, JE (2014) Postischemic reperfusion causes smooth muscle calcium sensitization and vasoconstriction of parenchymal arterioles. *Stroke* **45:** 2425-2430.

Demion, M, Bois, P, Launay, P, Guinamard, R (2007) TRPM4, a $Ca^{2+}$-activated nonselective cation channel in mouse sino-atrial node cells. *Cardiovasc Res* **73:** 531-538.

Dora, KA, Gallagher, NT, McNeish, A, Garland, CJ (2008) Modulation of endothelial cell $K_{Ca}3.1$ channels during endothelium-derived hyperpolarizing factor signaling in mesenteric resistance arteries. *Circ Res* **102:** 1247-1255.

Earley, S, Straub, SV, Brayden, JE (2007) Protein kinase C regulates vascular myogenic tone through activation of TRPM4. *Am J Physiol Heart Circ Physiol* **292:** H2613-2622.

Earley, S, Waldron, BJ, Brayden, JE (2004) Critical role for transient receptor potential channel TRPM4 in myogenic constriction of cerebral arteries. *Circ Res* **95:** 922-929.

Garland, CJ, Hiley, CR, Dora, KA (2011a) EDHF: spreading the influence of the endothelium. *Br J Pharmacol* **164:** 839-852.

Garland, CJ, McPherson, GA (1992) Evidence that nitric oxide does not mediate the hyperpolarization and relaxation to acetylcholine in the rat small mesenteric artery. *Br J Pharmacol* **105:** 429-435.

Garland, CJ, Yarova, PL, Jimenez-Altayo, F, Dora, KA (2011b) Vascular hyperpolarization to β-adrenoceptor agonists evokes spreading dilatation in rat isolated mesenteric arteries. *Br J Pharmacol* **164:** 913-921.

Gonzales, AL, Garcia, ZI, Amberg, GC, Earley, S (2010) Pharmacological inhibition of TRPM4 hyperpolarizes vascular smooth muscle. *Am J Physiol Cell Physiol* **299:** C1195-1202.

Grand, T, Demion, M, Norez, C, Mettey, Y, Launay, P, Becq, F, Bois, P, Guinamard, R (2008) 9-phenanthrol inhibits human TRPM4 but not TRPM5 cationic channels. *Br J Pharmacol* **153:** 1697-1705.

Guinamard, R, Hof, T, Del Negro, CA (2014) The TRPM4 channel inhibitor 9-phenanthrol. *Br J Pharmacol* **171:** 1600-1613.

Kansui, Y, Garland, CJ, Dora, KA (2008) Enhanced spontaneous $Ca^{2+}$ events in endothelial cells reflect signalling through myoendothelial gap junctions in pressurized mesenteric arteries. *Cell Calcium* **44:** 135-146.

McNeish, AJ, Sandow, SL, Neylon, CB, Chen, MX, Dora, KA, Garland, CJ (2006) Evidence for involvement of both $IK_{Ca}$ and $SK_{Ca}$ channels in hyperpolarizing responses of the rat middle cerebral artery. *Stroke* **37:** 1277-1282.

Nilius, B, Prenen, J, Tang, J, Wang, C, Owsianik, G, Janssens, A, Voets, T, Zhu, MX (2005) Regulation of the $Ca^{2+}$ sensitivity of the nonselective cation channel TRPM4. *J Biol Chem* **280:** 6423-6433.

Sala-Rabanal, M, Wang, S, Nichols, CG (2012) On potential interactions between non-selective cation channel TRPM4 and sulfonylurea receptor SUR1. *J Biol Chem* **287:** 8746-8756.

Tosun, C, Kurland, DB, Mehta, R, Castellani, RJ, deJong, JL, Kwon, MS, Woo, SK, Gerzanich, V, Simard, JM (2013) Inhibition of the SUR1-TRPM4 channel reduces neuroinflammation and cognitive impairment in subarachnoid hemorrhage. *Stroke* **44:** 3522-3528.

Wang, BH, Ternai, B, Polya, GM (1994) Specific inhibition of cyclic AMP-dependent protein kinase by the antimalarial halofantrine and by related phenanthrenes. *Biol Chem Hoppe Seyler* **375:** 527-535.

Weston, AH, Egner, I, Dong, Y, Porter, EL, Heagerty, AM, Edwards, G (2013) Stimulated release of a hyperpolarizing factor (ADHF) from mesenteric artery perivascular adipose tissue: involvement of myocyte $BK_{Ca}$ channels and adiponectin. *Br J Pharmacol* **169:** 1500-1509.

Woo, SK, Kwon, MS, Ivanov, A, Gerzanich, V, Simard, JM (2013) The sulfonylurea receptor 1 (SUR1)-transient receptor potential melastatin 4 (TRPM4) channel. *J Biol Chem* **288:** 3655-3667.

Wulff, H, Kohler, R (2013) Endothelial small-conductance and intermediate-conductance $K_{Ca}$ channels: an update on their pharmacology and usefulness as cardiovascular targets. *J Cardiovasc Pharmacol* **61:** 102-112.

Yamamoto, Y, Suzuki, H (2005) Dependency of endothelial cell function on vascular smooth muscle cells in guinea-pig mesenteric arteries and arterioles. *J Smooth Muscle Res* **41:** 77-85.

Yuill, KH, Yarova, P, Kemp-Harper, BK, Garland, CJ, Dora, KA (2011) A novel role for HNO in local and spreading vasodilatation in rat mesenteric resistance arteries. *Antioxid Redox Signal* **14:** 1625-1635.

***Figure Legends***

Figure 1.

Effect of 9-phenanthrol on the smooth muscle membrane potential of mesenteric arteries and block with TRAM-34. Panel A, (i-ii) intracellular records showing reproducible and reversible hyperpolarization to 20 μM 9-phenanthol (9-PA) in the same preparation (iii) which, in a separate preparation, was unaffected by the presence of 100 nM apamin, (iv) but blocked in the additional presence of 1 μM TRAM-34. Under these conditions, hyperpolarization was subsequently evoked with 5 μM levcromakalim (LVK). Panel B-D, box and whisker plots summarizing (B) the effect of 20 μM 9-phenanthrol against resting membrane potential (RMP, left panel, n=10) and in the presence of 5 μM glibenclamide (Glib, n=5), (C) lack of block with 100 nM apamin alone and block with 1 μM TRAM-34 alone (n=4 in each case), (D) the effect of $[Na^+]_o$ replacement with NMDG on the resting membrane potential (n=10). *, $P < 0.05$ *vs* RMP; $^{\#}$, $P < 0.05$ *vs* Control 9-PA.

Figure 2.

Damage to the endothelium (-EC) abolished hyperpolarization to acetylcholine and 9-phenanthrol but not to levcromakalim. Panel A, intracellular recording showing no hyperpolarization to 0.1 – 3 μM acetylcholine (ACh) or 20 μM 9-phenanthrol (9-PA), while the addition of the $K_{ATP}$ channel activator, 5 μM levcromakalim (LVK) evoked pronounced hyperpolarization to *circa* $E_K$. Panel B, concentration-response curves showing control contraction to phenylephrine (PE) is abolished in the presence of 20 μM 9-phenanthrol but reestablished in endothelium-damaged arteries in the presence of 9-phenanthrol (n=3 in each case). *, $P < 0.05$ *vs* Control.

Figure 3.

Measurement of endothelial cell calcium events and active cells in pressurized mesenteric arteries. 20 μM 9-phenanthrol (9-PA) did not alter basal $Ca^{2+}$ event frequency or the number of active cells, but blocked the ability of 0.3 μM ACh to stimulate events (n=3). *, $P < 0.05$ *vs* Basal.

Figure 4.

Current clamp recording from dispersed mesenteric artery EC sheets. Panel A, original trace showing reproducible and reversible hyperpolarization to 5 μM 9-phenanthrol, reduced in the presence of 1 μM TRAM-34. Panel B, box and whisker plot of paired data summarizing hyperpolarization to 5 μM 9-phenanthrol and reduced hyperpolarization (right panel) in the presence of 1 μM TRAM-34 (n=4 EC sheets). Panel C, summary of the hyperpolarization to superfusate containing NMDG (n=11 EC sheets). *, $P < 0.05$ *vs* RMP; $^{\#}$, $P < 0.05$ *vs* Control 9-PA.

Figure 5.

Confocal imaging in pressurized mesenteric arteries indicating TRPM4 antibody in endothelium and adventitia. **i.** Transmitted light image showing the relative alignment of endothelial cells (EC) and smooth muscle cells (SMC). Nuclear labelling (blue) with propidium iodide. **ii.** A merged image from the same artery (of five 0.5-μm z-axis planes) at the level of the internal elastic lamina (Elastin, white), focal plane EC in panel v. **iii.** Diffuse expression of TRPM4 (yellow) is apparent in the endothelium but absent from the SMCs. **iv.** Subsequent immunolabelling of the same artery for connexin 40 (yellow) using the same settings as iii, was restricted mainly to EC borders. **v.** Cartoon indicating the focal plane imaged for endothelial cells (EC) and shown in panels i-iv, and for adventitia shown in panel viii. **vi.** Reconstructed z-stacks, luminal surface upmost, showing alignment of SMCs approximately at right angles to the overlying ECs. **vii.** The same reconstructed z-stack including signal (yellow) indicating TRPM4 in the endothelium but absent from the SMC. **viii.** TRPM4 was also apparent at the level of the adventitia. Scale bar 50 μm applicable to all images. The pink asterisk marks the same nucleus in panels i-iv and vi-viii.

Figure 6.

Inhibition of 9-phenanthrol hyperpolarization and vasodilation in middle cerebral arteries by TRAM-34. Panel A, intracellular recording of smooth muscle membrane potential in a tensioned middle cerebral artery. Spontaneous depolarization and contraction is blocked with 1 μM nifedipine. 20 μM 9-phenanthrol then causes hyperpolarization. Panel B, box and whisker plot to summarize the ability of 20 μM 9-phenanthrol to raise membrane potential (left panel), and (right) reduced in the presence of 1 μM TRAM-34, n=4. Panel C, vasodilation to 20 μM 9-phenanthrol in pressurized cerebral arteries is slowed but not diminished by the presence of 1 μM TRAM-34, n=3. *, $P < 0.05$ *vs* RMP.